Stagnation Point Flow of Micropolar Maxwell Fluid over Riga Plate under the Influence of Heat and Mass Transfer

S. Nadeem[1], Asma Amin[1], Nadeem Abbas[1], Anber Saleem[2,3], Fahad M. Alharbi[4], Anwar Hussain[1], Alibek Issakhov[5]*

Abstract

In this paper, we investigated the stagnation point flow of Maxwell viscoelasticity with incompressible based micropolar fluid over a Riga plate. The mathematical model has been constructed though micropolar fluid flows over Riga plate. The implement the boundary layer approximation, the system of partial differential equations is produced through momentum equation along with micro inertia theory. Nonlinear partial differential equations are become dimensionless nonlinear ordinary differential equations through suitable similarity transformations. This system is solved numerical scheme via BVP4C method. The effects of involving physical parameters like as dimensionless parameter, Modified Hartman number, Material parameter, Slip condition σ_s, Viscoelastic parameter δ_m and Soret coefficient S_T are highlighted through graphs and numerical results. The physical quantities like as Skin friction, local Nusselt number and local Sher-wood number are highlighted through tables. R is increasing with increasing dimensionless parameter, Material parameter K and Slip condition σ_s. R is decreasing with increasing behavior of Modified Hartman number Z and viscoelastic parameter δ_m.

Keywords: Micropolar viscoelasticity fluid; Multi-dependent thermophoresis; Stagnation point flow; Riga plate; Numerical technique.

1. Introduction

Micropolar fluid analysis is the remarkable importance in the field of engineering and industrial process. Micropolar fluid offers high resistance to the fluid motion as compared to the Newtonian fluids. Due to lots of its applications, many investigators are interested to analyze the Micropolar fluid having different assumptions. At the early time, Lukaszewicz [1] was studying

[1] *Department of Mathematics, Quaid-I-Azam University 45320, Islamabad 44000, Pakistan.*
[2] *Mathematics and its Applications in Life Sciences Research Group, Ton Duc Thang University, Ho Chi Minh City, Vietnam.*
[3] *Faculty of Mathematics and Statistics, Ton Duc Thang University, Ho Chi Minh City, Vietnam.*
[4] *Department of Mathematics, Faculty of Science, University of Tabuk, P.O.Box 741, Tabuk 71491, Saudi Arabia*
[5] Al-Farabi Kazakh National University, av. al-Farabi 71, 050040, Almaty, Kazakhstan
**Corresponding author email: Anber Saleem (anber.saleem@tdtu.edu.vn)*

the micropolar fluid theory and its applications. Eringen [2] was extended the idea of Lukaszewicz [1]. He introduced the Microcontinuum field theory of the micropolar fluids. Several classical concepts like as absence of the couple stress or symmetry of the stress tensor are never larger occurred. Due to its relative simplicity of mathematics, the model of micropolar fluid have been extensively utilized in lubricant to analyze the polymer clarifications in which the viscous fluid lubricant is merged having less quantity of long chained added substances. Wang and Zhu [3] were highlighted the effects of lubricating on the micropolar fluid. They analyzed the basic theory of micropolar fluid and derived the modified Reynolds equation for dynamics loads. Several investigators are studied the micropolar fluids extensively on the different points of views because lots of its applications. Nadeem et al. [4] gained the numerical and exact solutions of micropolar fluids at vertical annulus. Hussain et al. [5] have been studied the micropolar fluid at stretching sheet. Heat and mass transfer of based micropolar fluid at permeable walls discussed by Ellahi et al. [6]. Rawi et al. [7] have been discussed the mixed convection flow with heat transfer of micropolar nanofluid. Abbas et al. [8] analyzed the based nanomaterial micropolar fluid at cylinder. They also discussed the effects of thermal slip and velocity slip on micropolar nanofluid. Nadeem et al. [9] have discussed the micropolar fluid at Riga plate. Many researchers are interested to study the micropolar fluid for different physical parameters see Refs. [10-13].

The flow of fluid is electrically conducting which can be controlled through electromagnetic forces. In any case, the speed of liquids having tall electrical conductivity can be controlled through more often than not attractive hydrodynamics flow control. The current initiated through outside attractive field alone are exceptionally little in case of feebly conducting liquid whereas the outside electric field must be connected to pick up an effective stream control. Gailitis and Lielausis [14] were pioneered of Riga plate. They introduced a device, namely Riga plate to create crossed magnetic and electric fields. Grinberg [15] was discussed the characteristics few potential fields. Grinberg [15] showing the divider parallel Lorentz drive within the boundary layer force condition is completely decoupled from the stream with opposite to the Hartmann term. It declines exponentially along normal to the plate. Pantokratoras and Magyari [16] were discussed the boundary layer flow over Riga plate. Magyari and Pantokratoras [17] studied the opposing and aiding mixed convection flow over Riga plate. Ayub et al [18] highlighted the blasius flow at Riga plate under the for modified Hartmann number. Ramzan et al. [19]

considered the impacts of nanomaterial micropolar fluid flow at Riga plate. The mixed convective condition with micropolar fluid flow ar Riga plate studied by Zaib et al. [20]. The convective boundary conditions and chemical radiations on the Riga plate discussed by Rasool and Zhang [21]. few analysts centered on the Riga plate since parts of its applications within the areas of engineering which see in Refs. [22-27].

Hiemenz [28] was the first one who introduced stagnation flow to gain exact solution of the Navier –Stokes equations. Howarth [29] worked out on the Hiemenz [28] idea and found best solution approximations. Ishak et al. [30] studied the boundary layer flow with the magnetic field effects under stagnation point region. Gorder and Vajravelu [31] discussed stagnation point flow of second grade fluid over stretching surface. Fang et al [32] investigated the unsteady stagnation point flow with mass transfer. Recent studied on the stagnation point flows are highlighted in the Refs. [33-41].

The aim of the this analysis, we investigated the stagnation point flow of Maxwell viscoelasticity with incompressible based micropolar fluid over a Riga plate. The mathematical model has been constructed though micropolar fluid flows over Riga plate. The implement the boundary layer approximation, the system of partial differential equations is produced through momentum equation along with micro inertia theory. Nonlinear partial differential equations are become dimensionless nonlinear ordinary differential equations through suitable similarity transformations. This system is solved numerical scheme via BVP4C method. Analysis of physical parameters on the Riga plate results is highlighted in form of tables and graphs.

2. Formulation of flow

We assume the two-dimensional Maxwell viscoelasticity-based micropolar fluid (MVMF) under the stagnation point at a horizontal Riga plate with slip velocity condition which reveals in **Fig. 1**. The plate in the direction of x-axis as well as normal to plate id y-axis. We consider that linear velocity at wall $U_w = ax$ and positive constant a . Flow model in the mathematics form as

$$\frac{\partial u}{\partial x} + \frac{\partial v}{\partial y} = 0, \tag{1}$$

$$u\frac{\partial u}{\partial x}+v\frac{\partial u}{\partial y}=\lambda\bar{U}_e^2\frac{d^2\bar{U}_e}{d\bar{x}^2}+\bar{U}_e\frac{d\bar{U}_e}{d\bar{x}}+\left(\frac{\mu+\kappa}{\rho}\right)\frac{\partial}{\partial y}\left(\frac{\partial u}{\partial y}\right)$$
$$-\lambda\left(u^2\frac{\partial^2 u}{\partial x^2}+v^2\frac{\partial^2 u}{\partial y^2}+2uv\frac{\partial^2 u}{\partial x\partial y}\right)+\frac{\kappa}{\rho}\frac{\partial N}{\partial y}+\frac{\pi j_0 M_0}{8\rho}e^{\frac{-\pi}{b}y}, \quad (2)$$

Where, the free steam velocity is $U_e=\omega x$ and ω is the positive constant.

$$u\frac{\partial u}{\partial x}+v\frac{\partial u}{\partial y}=\omega^2 x+\left(\frac{\mu+\kappa}{\rho}\right)\frac{\partial}{\partial y}\left(\frac{\partial u}{\partial y}\right)-\lambda\left(u^2\frac{\partial^2 u}{\partial x^2}+v^2\frac{\partial^2 u}{\partial y^2}+2uv\frac{\partial^2 u}{\partial x\partial y}\right)+\frac{\kappa}{\rho}\frac{\partial N}{\partial y}$$
$$+\frac{\pi j_0 M_0}{8\rho}e^{\frac{-\pi}{b}y}, \quad (3)$$

$$\rho j\left(u\frac{\partial N}{\partial x}+v\frac{\partial N}{\partial y}\right)=\frac{\partial}{\partial y}\left(\gamma\frac{\partial N}{\partial y}\right)-\kappa\left(2N+\frac{\partial u}{\partial y}\right), \quad (4)$$

Here, u and v are axial and transverse velocity components respectively. μ is dynamic viscosity, κ is gyro-viscosity or vortex viscosity, ρ is density of fluid, N is micro-angular velocity and rotation is normal to plate along $x-y$ plane, $\lambda=\frac{\alpha}{\rho}$ is relaxation time (T), in which α is the thermal diffusivity, M_0 is permanent magnets namely magnetization, j_0 current density, b is electrodes and magnet width, j micro-inertia per unit mass, $\left(j=\frac{\nu}{\omega}\right)$ and γ spin gradient viscosity which represents the relationship between μ and j, it can be written as

$$\gamma=\left(\mu+\frac{\kappa}{2}\right)j=\mu\left(1+\frac{K}{2}\right)j, \quad (5)$$

Here $K=\frac{\kappa}{\mu}$ represents dimensionaless ratio of viscosity and known as MVMF material parameter. The slip boundary at the surface is defined as

$$u=u_w+u_{slip}, v=0, N=-m\frac{\partial u}{\partial y} \quad \text{at} \quad y=0, \quad (6)$$

which the condition at infinity is defined as

$$u\to U_e=\omega x, N\to 0 \quad \text{as} \quad y\to\infty, \quad (7)$$

Where u_{slip} is the slip velocity which is defined as $u_{slip}=L\left[(1+K)\frac{\partial u}{\partial y}+KN\right]_{y=0}$ in which $L=l\mu$ is a positive constant, m is a constant lies between 0 and 1, where $m=0$ indicates the

concentrated MVMF and $m=1$ represents turbulent flow circumstance. In our case we use $m=\frac{1}{2}$ to define a *dilute* MVMF.

3. Mathematical model of heat and mass transfer

We suppose that surface temperature of the Riga plate is T_w while temperature in free-stream condition also known as ambient temperature is T_∞, where $T_w > T_\infty$. Here C_w is the concentration of plate at surface and C_∞ is ambient concentration. By using assumptions given above and boundary layer principle, we obtain conservations equations of energy and concentration equation for MVMF.

$$u\frac{\partial T}{\partial x}+v\frac{\partial T}{\partial y}=\frac{k}{\rho C_p}\frac{\partial^2 T}{\partial y^2}+\frac{k_T D_m}{C_s C_p}\frac{\partial^2 C}{\partial y^2}+\frac{\mu_B+\kappa}{\rho C_p}\left(\frac{\partial u}{\partial y}\right)^2, \tag{8}$$

$$u\frac{\partial C}{\partial x}+v\frac{\partial C}{\partial y}=D_m\frac{\partial^2 C}{\partial y^2}+\frac{k_T D_m}{T_m}\frac{\partial^2 T}{\partial y^2}, \tag{9}$$

corresponding boundary conditions are following

$$T=T_w, C=C_w \quad \text{at} \quad y=0, \tag{10}$$

$$T=T_\infty, C=C_\infty \quad \text{as} \quad y\to\infty, \tag{11}$$

Where,

k	Thermal conductivity of the fluid	C_s	Concentration susceptibility
D_m	Mass diffusivity	k_T	Thermal diffusion ratio
T_m	Fluid temperature across boundary layer	C_p	Specific heat capacity

The second term on right side Dufour effect in Eq. (8) and Eq. (9) soret effect that play significant role on temperature distribution and concentration distribution in MVMF.

4. Similarity transformation equation

We have introduced the following suitable similarity transformation are

$$\psi=(\omega\nu)^{\frac{1}{2}}xf(\eta), \quad \eta=\left(\frac{\omega}{\nu}\right)^{\frac{1}{2}}y, \quad N=\left(\frac{\omega^3}{\nu}\right)^{\frac{1}{2}}xR, \tag{12}$$

$$\theta=\frac{T-T_\infty}{T_w-T_\infty}, \quad \phi=\frac{C-C_\infty}{C_w-C_\infty}, \tag{13}$$

Where ψ the stream function and velocity components are expressed as

$$u = \frac{\partial \psi}{\partial y}, v = -\frac{\partial \psi}{\partial x}, \tag{14}$$

η is non-dimensional parameter, R is non-dimensional local microvelocity, $\nu = \frac{\mu}{\rho}$ kinematic viscosity, θ is the normalized temperature and ϕ is normalized concentration. By means of similarity transformation equations, PDEs (3)-(4) and (8)-(9) are diminished as follows below:

$$(1+K) f''' + ff'' - (f')^2 - \delta_m \left(1 + f^2 f''' - 2ff'f''\right) + KR' + Ze^{-d\eta} + 1 = 0, \tag{15}$$

$$\left(1 + \frac{K}{2}\right) R'' + fR' - f'R - K(2R + f'') = 0, \tag{16}$$

$$\frac{1}{Pr}\theta'' + f\theta' + Du\phi'' + Gb(1+K)(f'')^2 = 0, \tag{17}$$

$$\phi'' + Sc(f\phi' + Sr\theta'') = 0, \tag{18}$$

Corresponding non-dimensional boundary conditions are

$$f(0) = 0, \quad f'(0) = S + \sigma_s \left(1 + \frac{K}{2}\right) f''(0), \quad R(0) = -\frac{f''(0)}{2}, \tag{19}$$

$$\theta(0) = 1, \quad \phi(0) = 1, \tag{20}$$

$$f'(\infty) = 1, \quad R(\infty) = 0, \quad \theta(\infty) = 0, \quad \phi(\infty) = 0, \tag{21}$$

Here prime rpresents derivative w r t η. $\delta_m = \lambda\omega$ denotes the non-dimensional viscoelastic parameter , Pr is Prandtl number, $Pr = \frac{\mu C_p}{\kappa}$, σ_s is the slip velocity parameter, $\sigma_s = l(\rho\mu\omega)^{\frac{1}{2}}$, Gebhart number, define as Gb, Sc Schmidt number, $Sc = \frac{\nu}{D_m}$, Du is the Dufour number, $Du = \frac{k_T D_m (C_w - C_\infty)}{C_s C_p \nu (T_w - T_\infty)}$, Sr Soret number, define as, $Sr = \frac{k_T D_m (T_w - T_\infty)}{T_m \nu (C_w - C_\infty)}$, Z is the Modified Hartman number, define as, $Z = \frac{\pi j_0 M_0 x}{8\rho U_e^2}$, d dimensionless parameter, $d = \frac{\pi}{b}\sqrt{\frac{\nu}{\omega}}$. For stretching $\left(S = \frac{a}{\omega} > 0\right)$ and for shrinking $\left(S = \frac{a}{\omega} < 0\right)$.

S	stretching/shrinking parameter	Z	Modified Hartman number
β	dimensionless parameter	K	Material parameter
δ_m	Viscoelastic parameter	σ_s	Slip condition

The normalized velocity is $f' = \frac{u}{U_e}$, and the physical quantities in engineering applications are defined as

$$C_f = \frac{\tau_w}{\rho U_e^2}, \quad Nu_x = \frac{xq_w}{k(T_w - T_\infty)}, \quad Sh_x = \frac{xJ_w}{D_m(C_w - C_\infty)}, \tag{22}$$

Where C_f is the skin friction, Nu_x is the local Nusselt number and Sh_x is local Sher-wood number for transfer of mass. τ_w is the wall shear stress of MVMF, q_w is wall heat current and J_w is wall mass current, which are defined as

$$\tau_w = -\mu(1+\delta_m)\left[(1+K)\frac{\partial u}{\partial y} + KN\right]_{y=0}, \tag{23}$$

$$q_w = -k\left(\frac{\partial T}{\partial y}\right)_{y=0}, \quad J_w = -D_m\left(\frac{\partial C}{\partial y}\right)_{y=0}, \tag{24}$$

Using similarity variables, we can obtain the non-dimensional engineering parameters as

$$Re^{-\frac{1}{2}}C_f = -(1+\delta_m)\left(1+\frac{K}{2}\right)f''(0), \quad Re^{-\frac{1}{2}}Nu_x = -\theta'(0), \quad Re^{-\frac{1}{2}}Sh_x = -\phi'(0), \tag{25}$$

Where $Re = \frac{U_e x}{\nu}$ is the Reynolds number.

5 Numerical procedure

We decreased the higher order differential system within the initial value issue. The method of the numerical procedure is characterized underneath:

$$q(1) = f(\eta), q(2) = f'(\eta), q(3) = f''(\eta), qq1 = f'''(\eta),$$
$$q(4) = R(\eta), q(5) = R'(\eta), qq2 = R''(\eta), q(6) = \theta(\eta), q(7) = \theta'(\eta), qq3 = \theta''(\eta),$$
$$q(8) = \phi(\eta), q(9) = \phi'(\eta), qq4 = \phi''(\eta),$$
$$qq1 = -\left(1+K-\delta_m q(1)q(1)\right)^{-1}\begin{pmatrix} q(1)q(3) - q(2)q(2) - \delta_m\left(1-2q(1)q(2)q(3)\right) + Kq(5) \\ +Ze^{-dx} + 1 \end{pmatrix}$$
$$qq2 = -\left(1+\frac{K}{2}\right)^{-1}\left(q(1)q(5) - q(2)q(4) - K\left(2q(4) + q(3)\right)\right),$$
$$qq3 = -Pr\left(q(1)q(7) + Duqq4 + Gb(1+K)q(3)q(3)\right),$$
$$qq4 = Sc\left(q(1)q(9) + Srqq3\right),$$
$$q0(1); q0(2) - S - \sigma_s\left(1+\frac{K}{2}\right)q0(3); q0(4) + \frac{q0(3)}{2}; q0(6) - 1; q0(8) - 1;$$
$$qinf(2) - 1; qinf(4); qinf(6); qinf(8);$$

6 Result and discussion

The system of nonlinear ordinary differential conditions (15-18) with regard to the dimensionless boundary conditions (19-21) are illuminated by Numerical procedure reffered as BVP4C strategy to analyze the diverse physical parameters which highlighted through Figs (2-9).

6.1 Multi-dependent Soret number

Soret number or thermophoresis is dimensionless number applied to analyze the influence of temperature gradient on mass flux. Steady state concentration field in hard sphere particle suspensions is given by the equation:

$$D_m \frac{\nabla C}{C} = -D_T \nabla T, \tag{26}$$

This shows the thermophoresis velocity of particles denoted by v_T, in which D_T is called "thermal diffusion coefficient" (26-28). The Soret coefficient is defined as $S_T = \frac{D_T}{D_m}$ with dimension T^{-1} (27-28). The sign of Soret coefficient shows along the moving particles. If $S_T > 0$, the particles shows thermophobic behavior and if $S_T < 0$, they shows thermophilic behavior. Using the empirical expression of Soret coefficient S_T, the experimental results for particle radii at entire temperature range were fitted as

$$S_T(T) = S_T^{\infty}\left[1 - exp\left(\frac{T^* - T}{T_0}\right)\right], \tag{27}$$

Where S_T^{∞} is the reference value, T^* is the temperature, the Soret coefficient changes its sign and T_0 is the strength of the temperature impacts. Here, we take multidependent Soret number Sr which is an akin functional version to Soret coefficient. We consider the case where $Sr \rangle 0$, then T^* and T_0 should be replaced by T_∞ and T_w respectively. By using the transformation (12-13) in (26) and gained variable Soret number defined as

$$Sr = Sr_\infty\left[1 - exp\left(\theta\left(\frac{T_\infty}{T_w} - 1\right)\right)\right], \tag{28}$$

Where Sr_∞ is a positive coefficient and $0 < \frac{T_\infty}{T_w} < 1$ ensures $Sr > 0$. By using (27) in (18), we get

$$\phi'' + Sc\left(f\phi' + Sr_\infty\left[1 - exp\left(\theta\left(\frac{T_\infty}{T_w} - 1\right)\right)\right]\theta''\right) = 0, \tag{29}$$

The effects of Normalized velocity, Micro-angular velocity, Temperature profile and Concentration profile denoted by $f'(\eta), R(\eta), \theta(\eta)$ and $\phi(\eta)$ respectively will be examined by solving the equations (15)-(21).

6.2 Numerical results

The impacts of some physical quantities like Skin friction coefficients $Re^{\frac{1}{2}}C_f$, local Nusselt number $Re^{-\frac{1}{2}}Nu_x$ and local Sher-wood number $Re^{-\frac{1}{2}}Sh_x$ are shown in Table 1.The variation of different parameters such as, $S, K, \delta_m, \sigma_s, Du, Sc, Sr, Ec, Z$ and d on altere physical quantities $Re^{\frac{1}{2}}C_f$, $Re^{-\frac{1}{2}}Nu_x$ and $Re^{-\frac{1}{2}}Sh_x$ are highlighted in Table 1. For stretching parameter $(S>0)$, the values of $Re^{\frac{1}{2}}C_f$, $Re^{-\frac{1}{2}}Nu_x$ and $Re^{-\frac{1}{2}}Sh_x$ increases, however, for $(S<0)$, the values of $Re^{\frac{1}{2}}C_f$ and $Re^{-\frac{1}{2}}Nu_x$ increases while $Re^{-\frac{1}{2}}Sh_x$ decreases. For large values of K, the values of $Re^{\frac{1}{2}}C_f$ and $Re^{-\frac{1}{2}}Nu_x$ declines whereas the values of $Re^{-\frac{1}{2}}Sh_x$ rises. The values of all physical quantities $Re^{\frac{1}{2}}C_f$, $Re^{-\frac{1}{2}}Nu_x$and $Re^{-\frac{1}{2}}Sh_x$decreases for increasing values of δ_m. Both the values of $Re^{\frac{1}{2}}C_f$ and $Re^{-\frac{1}{2}}Nu_x$diensions while the values of $Re^{-\frac{1}{2}}Sh_x$ improves for larger values of Ec. For increasing values of Du and Sc, $Re^{\frac{1}{2}}C_f$, $Re^{-\frac{1}{2}}Nu_x$ and $Re^{-\frac{1}{2}}Sh_x$ have constant, decreasing and increasing behavior respectively. The behavior of $Re^{\frac{1}{2}}C_f$ and $Re^{-\frac{1}{2}}Nu_x$ is the same as Sr and σ_s but the behavior of $Re^{-\frac{1}{2}}Sh_x$ is opposite to the behavior of Sr and σ_s. Both the quantities $Re^{-\frac{1}{2}}Nu_x$ and $Re^{-\frac{1}{2}}Sh_x$ have the same nature as the nature of Z while $Re^{\frac{1}{2}}C_f$ has opposite nature. The values of $Re^{\frac{1}{2}}C_f$ and $Re^{-\frac{1}{2}}Nu_x$ increases as increase in the values of d but the values of and $Re^{-\frac{1}{2}}Sh_x$ dclines as increase in the values of d.

The dimensionless system (15-17) and (28) having dimensionless boundary conditions (19-21) are elucidated by BVP4C numerical scheme to investigate the physical parameters which are noted as multi dependent Soret number Sr_∞ and variable temperature difference $\frac{T_\infty}{T_w}$.The effect of different physical quantities such as Skin friction, Nusselt number and Sher-wood number are

emphasized in Table 2. The variation of $S, \frac{T_\infty}{T_w}, Sr_\infty, K, \delta_m, \sigma_s, Du, Sc, Sr, Ec, Z$ and d on $Re^{\frac{1}{2}}C_f$, $Re^{-\frac{1}{2}}Nu_x$ and $Re^{-\frac{1}{2}}Sh_x$ are shown in Table 2. For $(S>0)$, the values of $Re^{\frac{1}{2}}C_f$, $Re^{-\frac{1}{2}}Nu_x$ and $Re^{-\frac{1}{2}}Sh_x$ increases whereas for $(S<0)$, the values of $Re^{\frac{1}{2}}C_f, Re^{-\frac{1}{2}}Nu_x$ increases while the values of $Re^{-\frac{1}{2}}Sh_x$ decreases for increasing values of S .The values of $Re^{-\frac{1}{2}}Nu_x$ and $Re^{-\frac{1}{2}}Sh_x$ are increases for large values of $\frac{T_\infty}{T_w}$ whereas $Re^{\frac{1}{2}}C_f$ remain constant. The effects of Sr_∞ on $Re^{\frac{1}{2}}C_f$, $Re^{-\frac{1}{2}}Nu_x$ and $Re^{-\frac{1}{2}}Sh_x$ are highlighted in Table 2. It is famous that for higher values of Sr_∞, $Re^{-\frac{1}{2}}Nu_x$ and $Re^{-\frac{1}{2}}Sh_x$ have decreasing behavior whereas the values of $Re^{\frac{1}{2}}C_f$ remain constant. For increasing values of K, $Re^{\frac{1}{2}}C_f$ and $Re^{-\frac{1}{2}}Nu_x$ have decreasing behavior while $Re^{-\frac{1}{2}}Sh_x$ has opposite behavior which depicts in Table 2. The effects of δ_m on $Re^{\frac{1}{2}}C_f$, $Re^{-\frac{1}{2}}Nu_x$ and $Re^{-\frac{1}{2}}Sh_x$ are shown in Table 2. For large values of δ_m, $Re^{\frac{1}{2}}C_f$, $Re^{-\frac{1}{2}}Nu_x$ and $Re^{-\frac{1}{2}}Sh_x$ have decreasing behavior. The impacts of σ_s on $Re^{\frac{1}{2}}C_f$, $Re^{-\frac{1}{2}}Nu_x$ and $Re^{-\frac{1}{2}}Sh_x$ are shown in Table 2. It is perceived that the values of $Re^{\frac{1}{2}}C_f$ and $Re^{-\frac{1}{2}}Nu_x$ rises for rising behavior of σ_s while the values of $Re^{-\frac{1}{2}}Sh_x$ shows opposite behavior that decreases for large values of σ_s. Table 2 highlighted the effects of Du and Sc on $Re^{\frac{1}{2}}C_f$, $Re^{-\frac{1}{2}}Nu_x$ and $Re^{-\frac{1}{2}}Sh_x$. It is depicted that the behavior of $Re^{\frac{1}{2}}C_f$ is constant while $Re^{-\frac{1}{2}}Nu_x$ and $Re^{-\frac{1}{2}}Sh_x$ have opposite behavior to each other that $Re^{-\frac{1}{2}}Nu_x$ decreases and $Re^{-\frac{1}{2}}Sh_x$ growths for increasing values of Du and Sc. For large values of Sr the behavior of $Re^{\frac{1}{2}}C_f$, $Re^{-\frac{1}{2}}Nu_x$ and $Re^{-\frac{1}{2}}Sh_x$ revealed in Table 2. It is also note that $Re^{\frac{1}{2}}C_f$ and $Re^{-\frac{1}{2}}Nu_x$ increases whereas $Re^{-\frac{1}{2}}Sh_x$ declines for great values of Sr. Table

2 depicts the impacts of Gb on physical quantities $Re^{\frac{1}{2}}C_f$, $Re^{-\frac{1}{2}}Nu_x$ and $Re^{-\frac{1}{2}}Sh_x$. For increasing behavior of Gb, $Re^{\frac{1}{2}}C_f$ and $Re^{-\frac{1}{2}}Nu_x$ shows decreasing behavior, however $Re^{-\frac{1}{2}}Sh_x$ shows increasing behavior. Table 2 highlighted the effects of Z on $Re^{\frac{1}{2}}C_f$, $Re^{-\frac{1}{2}}Nu_x$ and $Re^{-\frac{1}{2}}Sh_x$. It is observed that both $Re^{-\frac{1}{2}}Nu_x$ and $Re^{-\frac{1}{2}}Sh_x$ increases whereas $Re^{\frac{1}{2}}C_f$ decreases for growing values of Z. The values of $Re^{\frac{1}{2}}C_f$ and $Re^{-\frac{1}{2}}Nu_x$ surges for higher values of d however the values of $Re^{-\frac{1}{2}}Sh_x$ decreases which shown in Table 2.

6.3 Graphical Results

Figs (2-11) shows the effects of different physical parameters such as dimensionless parameter β , Modified Hartman number Z , Material parameter K , Slip condition σ_s , Viscoelastic parameter δ_m , Multi dependent Soret number Sr_∞ and Variable temperature difference $\frac{T_\infty}{T_w}$ on Normalized fluid velocity $\left(\frac{u}{U_e}\right)$, Micro-angular velocity (R) , Temperature profile (θ) and Concentration profile (ϕ). Figs. [2(a)-2(b)] demonstrate the impact of viscoelastic parameter δ_m on $f' = \frac{u}{U_e}$ and ϕ. Both f' and ϕ increases for increase in the values of viscoelastic parameter δ_m. Figs. [3(a)-3(b)] depicts the impact of Slip condition σ_s on f' and ϕ respectively. It should be noted that f' increases as well as ϕ decreases for increasing values of Slip condition σ_s. Figs. [4(a)-4(b)] shows the impact of Material parameter K on f' and ϕ respectively. For increase in Material parameter, f' has decreasing behavior whereas ϕ has increasing behavior. Figs. [5(a)-5(b)] are highlighted the impact of Hartman number Z on f' and ϕ. It is perceived that f' growths while ϕ decreases as rise in the values of Hartman number Z. Figs. [6(a)-6(b)] depicts the impacts of dimensionless parameter β on f' and ϕ. It is observed that f' displays reducing behavior and ϕ shows increasing behavior for large values of dimensionless parameter β. Figs. [7(a)-7(b)] shows the impact of viscoelastic parameter δ_m and slip condition σ_s on R

and θ respectively. It is detected that R declines for growth in σ_s and increases for increase in δ_m while θ decreases for both viscoelastic parameter δ_m and Slip condition σ_s. The effects of Modified Hartman number Z on R and θ are highlighted in Fig. 8(a). For higher values of Z, it is perceived that R increases and θ decreases. Fig. 8(b) depicts the effects of dimensionless parameter β on R and θ. It is noted that R and θ shows opposite behavior that R decreases and θ increases. Fig. (9) shows the impact of Material parameter K on R and θ. It is also observed that θ shows same behavior as the behavior of K whereas R shows opposite behavior. Fig. (10) depicts the effect of Multi-dependent Soret number Sr_∞ on ϕ. It is perceived that ϕ increases as growth in Multi-dependent Soret number. The effect of Variable temperature difference $\frac{T_\infty}{T_w}$ on ϕ is highlighted in Fig. (11). It should be noted that the concentration profile and the Variable temperature difference have opposite behavior.

7 Conclusions

In this paper, we assume the two-dimensional Maxwell viscoelasticity-based micropolar fluid (MVMF) under the stagnation point at a horizontal Riga plate with slip velocity condition. We also discussed the impacts of different physical parameters and highlighted the results of these parameters. Some significant results are given below.

- θ and ϕ are increasing with increasing dimensionless parameter β and Material parameter K.
- θ and ϕ are decreasing for increasing values of Slip condition σ_s and Modified Hartman number Z.
- R is increasing with increasing dimensionless parameter , Material parameter K and Slip condition σ_s.
- R is decreasing with increasing behavior of Modified Hartman number Z and viscoelastic parameter δ_m.

Author biographies

Sohail Nadeem is working as Professor/Chairman at the Department of Mathematics at Quaid-i-Azam University, Islamabad, Pakistan. More than 25 PhD scholars and more than 100 M. Phil students have completed their respective degrees under his supervision. He has published more than 500 research articles in well reputed international journals, having more than 7000 citations.

He has been awarded several national/international awards. He is also a member of several editorial boards in well reputed international journals. Nationally, he is serving on with several scientic committees throughout the country.

Asma Amin was born in Rawalpindi, Punjab, Pakistan. He obtained his MPhil degrees from the Department of Mathematics at Quaid-iAzam University, Islamabad, Pakistan, and is currently working as lecturere in the Department of Mathematics at HITEC University, Taxila Cantt, Rawalpindi, Punjab, Pakistan. She published her work in the ineternational well reputed impact factor journal.

Nadeem Abbas was born on September 15, 1990 in District Jhang, Punjab, Pakistan. He earned his MS degree in Mathematics in 2014 from the University of the Punjab Lahore, Pakistan and a M. Phil and Ph.D degree from Quaid-i-Azam University Islamabad, Pakistan. Now, he is working as Assistant Professor in the department of Mathematics, Riphah International University, Faisalabad Campus, Faisalabad, Pakistan. He has published more than 30 research articles in well reputed international journals, having more than 470 citations.

Anber Saleem is working as Professor at the Department of 3Islamabad Medical and Dental College, Islamabad, Pakistan. She has published more than 50 research articles in well reputed international journals, having more than 500 citations. She is also a member of several editorial boards in well reputed international journals. Nationally, he is serving on with several scientic committees throughout the country.

Fahad M. Alharbi is working as Assistant professor in department of Mathematics, Faculty of Science, University of Tabuk, Tabuk, Saudi Arabia. Nationally, he is serving on with several scientic committees throughout the country. He has published more than 50 research articles in well reputed international journals, having more than 500 citations. He has been awarded several national/international awards. He is also a member of several editorial boards in well reputed international journals.

Anwar Hussain is working as Assistant professor in department of Mathematics, Quaid-i-Azam University Islamabad, Pakistan. Nationally, he is serving on with several scientic committees throughout the country. He has published more than 40 research articles in well reputed international journals, having more than 500 citations. He has been awarded several national/international awards. Nationally, he is serving on with several scientic committees throughout the country.

Alibek Issakhov Alharbi is working as professor in department of Mathematics Al-Farabi Kazakh National University, av. al-Farabi, Almaty, Kazakhstan. Nationally, he is serving on with several scientic committees throughout the country. He has published more than 25 research articles in well reputed international journals, having more than 1000 citations. He has been awarded several national/international awards. He is also a member of several editorial boards in well reputed international journals.

References

1 Lukaszewicz, G. Micropolar fluids: theory and applications. *Springer Science & Business Media, (1999).*

2 Eringen, A. C. Microcontinuum field theories: II. Fluent media (Vol. 2). *Springer Science & Business Media, (2001).*

3 Wang, X. L., & Zhu, K. Q. A study of the lubricating effectiveness of micropolar fluids in a dynamically loaded journal bearing (T1516). *Tribology International, 37(6), 481-490, (2004).*

4 Nadeem, S., Akbar, N. S., & Malik, M. Y. Exact and numerical solutions of a micropolar fluid in a vertical annulus. *Numerical Methods for Partial Differential Equations, 26(6), 1660-1674, (2010).*

5 Hussain, S. T., Nadeem, S., & Haq, R. U. Model-based analysis of micropolar nanofluid flow over a stretching surface. *The European Physical Journal Plus, 129(8), 161, (2014).*

6 Ellahi, R., Rahman, S. U., Nadeem, S., & Akbar, N. S. Influence of heat and mass transfer on micropolar fluid of blood flow through a tapered stenosed arteries with permeable walls. *Journal of Computational and Theoretical Nanoscience, 11(4), 1156-1163, (2014).*

7 Rawi, N. A., Ilias, M. R., Isa, Z. M., & Shafie, S. G-Jitter induced mixed convection flow and heat transfer of micropolar nanofluids flow over an inclined stretching sheet. *In AIP Conference Proceedings (Vol. 1775, No. 1, p. 030020). AIP Publishing, (2016).*

8 Abbas, N., Saleem, S., Nadeem, S., Alderremy, A. A., & Khan, A. U. On stagnation point flow of a micro polar nanofluid past a circular cylinder with velocity and thermal slip. *Results in Physics, 9, 1224-1232, (2018).*

9 Nadeem, S., Malik, M. Y., & Abbas, N. Heat transfer of three dimensional micropolar fluids on Riga plate. Canadian Journal of Physics, (*ja), (2019).*

10 Mollamahdi, M., Abbaszadeh, M., & Sheikhzadeh, G. A. Analytical study of Al2O3-Cu/water micropolar hybrid nanofluid in a porous channel with expanding/contracting walls in the presence of magnetic field. *Scientia Iranica*, 25(1), 208-220, (2018).

11 Nayak, M. K., Zeeshan, A., Pervaiz, Z., & Makinde, O. D. Modelling, Measurement and Control B. *Journal Homepage: http://iieta. org/journals/mmc_b*, *88(1), 33-41, (2019).*

12 Abro, K. A., & Yildirim, A. An analytic and mathematical synchronization of micropolar nanofluid by Caputo-Fabrizio approach. *Scientia Iranic*a, 26(6), 3917-3927, (2019).

13 Atif, S. M., Hussain, S., & Sagheer, M. Effect of thermal radiation on MHD micropolar Carreau nanofluid with viscous dissipation, Joule heating, and internal heating. *Scientia Iranica. Transaction F, Nanotechnology, 26(6), 3875-3888, (2019).*

14 Gailitis, A. K., & Lielausis, O. A. On the possibility of drag reduction of a flat plate in an electrolyte. Appl. Magnetohydrodyn. *Trudy Inst. Fisiky AN Latvia SSR, 12, 143, (1961).*

15 Grinberg, E. On determination of properties of some potential fields. *Applied Magnetohydrodynamics. Reports of the Physics Institute, 12, 147-154, (1961).*

16 Pantokratoras, A., & Magyari, E. EMHD free-convection boundary-layer flow from a Riga-plate. *Journal of Engineering Mathematics, 64(3), 303-315, (2009).*

17 Magyari, E., & Pantokratoras, A. Aiding and opposing mixed convection flows over the Riga-plate. *Communications in Nonlinear Science and Numerical Simulation, 16(8), 3158-3167, (2011).*

18 Ayub, M., Abbas, T., & Bhatti, M. M. Inspiration of slip effects on electromagnetohydrodynamics (EMHD) nanofluid flow through a horizontal Riga plate. *The European Physical Journal Plus, 131(6), 193, (2016).*

19 Ramzan, M., Bilal, M., & Chung, J. D. Radiative Williamson nanofluid flow over a convectively heated Riga plate with chemical reaction-A numerical approach. *Chinese Journal of Physics, 55(4), 1663-1673, (2017).*

20 Zaib, A., Haq, R. U., Chamkha, A. J., & Rashidi, M. M. Impact of partial slip on mixed convective flow towards a Riga plate comprising micropolar TiO2-kerosene/water nanoparticles. *International Journal of Numerical Methods for Heat & Fluid Flow, (2018).*

21 Rasool, G., & Zhang, T. Characteristics of chemical reaction and convective boundary conditions in Powell-Eyring nanofluid flow along a radiative Riga plate. *Heliyon, 5(4), e01479, (2019).*

22 Bhatti, M. M., Zeeshan, A., Ellahi, R., & Shit, G. C. Mathematical modeling of heat and mass transfer effects on MHD peristaltic propulsion of two-phase flow through a Darcy-Brinkman-Forchheimer porous medium. *Advanced Powder Technology, 29(5), 1189-1197, (2018).*

23 Nayak, M. K., Shaw, S., Makinde, O. D., & Chamkha, A. J. Effects of Homogenous–Heterogeneous reactions on radiative NaCl-CNP nanofluid flow past a convectively heated vertical Riga plate. *Journal of Nanofluids, 7(4), 657-667, (2018).*

24 Mehmood, R., Nayak, M. K., Akbar, N. S., & Makinde, O. D. Effects of thermal-diffusion and diffusion-thermo on oblique stagnation point flow of couple stress Casson fluid over a stretched horizontal Riga plate with higher order chemical reaction. *Journal of Nanofluids, 8(1), 94-102, (2019).*

25 Nayak, M. K., Shaw, S., Makinde, O. D., & Chamkha, A. J. Investigation of partial slip and viscous dissipation effects on the radiative tangent hyperbolic nanofluid flow past a vertical permeable Riga plate with internal heating: Bungiorno model. *Journal of Nanofluids, 8(1), 51-62, (2019).*

26 Riaz[1], A., Ellahi, R., Bhatti, M. M., & Marin, M. Study of Heat and Mass Transfer on Eyring-Powell Fluid Model Propagating Peristaltically through a Rectangular Complaint Channel, *DOI: 10.1615/HeatTransRes.2019025622, (2019).*

27 Khan, A. A., Bukhari, S. R., Marin, M., & Ellahi, R. Effects of chemical reaction on third-grade MHD fluid flow under the influence of heat and mass transfer with variable reactive index. *Heat Transfer Research, 50(11), (2019).*

28 Hiemenz, K. Die Grenzschicht an einem in den gleichformigen Flussigkeitsstrom eingetauchten geraden Kreiszylinder. *Dinglers Polytech. J., 326, 321-324, (1911).*

29 Howarth, L. CXLIV. The boundary layer in three dimensional flow.—Part II. The flow near a stagnation point. *The London, Edinburgh, and Dublin Philosophical Magazine and Journal of Science, 42(335), 1433-1440, (1951).*

30 Ishak, A., Jafar, K., Nazar, R., & Pop, I. MHD stagnation point flow towards a stretching sheet. *Physica A: Statistical Mechanics and its Applications, 388(17), 3377-3383, (2009).*

31 Van Gorder, R. A., & Vajravelu, K. Hydromagnetic stagnation point flow of a second grade fluid over a stretching sheet. *Mechanics Research Communications, 37(1), 113-118, (2011).*

32 Fang, T., Chia-fon, F. L., & Zhang, J. The boundary layers of an unsteady incompressible stagnation-point flow with mass transfer. *International Journal of Non-Linear Mechanics, 46(7), 942-948, (2011).*

33 Nadeem, S., Abbas, N., & Khan, A. U. Characteristics of three dimensional stagnation point flow of Hybrid nanofluid past a circular cylinder. *Results in Physics, 8, 829-835, (2018).*

34 Nadeem, S., & Abbas, N. On both MHD and slip effect in Micropolar hybrid nanofluid past a circular cylinder under stagnation point region. *Canadian Journal of Physics, (ja), (2018).*

35 Iacopini, S., & Piazza, R. Thermophoresis in protein solutions. *EPL (Europhysics Letters), 63(2), 247, (2003)*.

36 Putnam, S. A., Cahill, D. G., & Wong, G. C. Temperature dependence of thermodiffusion in aqueous suspensions of charged nanoparticles. *Langmuir, 23(18), 9221-9228, (2007).*

37 Braibanti, M., Vigolo, D., & Piazza, R. Does thermophoretic mobility depend on particle size. *Physical Review Letters, 100(10), 108303. (2008).*

38 Khan, A. A., Usman, H., Vafai, K., & Ellahi, R. Study of peristaltic flow of magnetohydrodynamics Walter's B fluid with slip and heat transfer. *Scientia Iranica, 23(6), 2650-2662,(2016).*

39 Niranjan, H., Sivasankaran, S., & Bhuvaneswari, M. Chemical reaction, Soret and Dufour effects on MHD mixed convection stagnation point flow with radiation and slip condition. *Scientia Iranica. Transaction B, Mechanical Engineering, 24(2), 698, (2017).*

40 Ijaz, N., Zeeshan, A., Bhatti, M. M., & Ellahi, R. Analytical study on liquid-solid particles interaction in the presence of heat and mass transfer through a wavy channel. *Journal of Molecular Liquids, 250, 80-87, (2018).*

41 Nayak, M. K., Hakeem, A. K., & Makinde, O. D. Influence of Catteneo-Christov Heat Flux Model on Mixed Convection Flow of Third Grade Nanofluid over an Inclined Stretched Riga Plate. *In Defect and Diffusion Forum (Vol. 387, pp. 121-134). Trans Tech Publications Ltd, (2018).*

Table 1: Numerical values of skin friction, local Nusselt number and local Sher-wood

S	K	δ_m	σ_s	Du	Sc	Sr	Gb	Z	d	$Re^{\frac{1}{2}}C_f$	$Re^{-\frac{1}{2}}Nu_x$	$Re^{-\frac{1}{2}}Sh_x$
-0.3	0.6	0.4	0.5	0.3	0.5	0.4	0.3	0.7	0.9	-2.1853	0.4554	0.5422
-0.2										-2.0684	0.5306	0.5359
-0.1										-1.9627	0.5955	0.5342
0.0										-1.8563	0.6561	0.5335
0.1										-1.7497	0.7124	0.5337
0.2										-1.6276	0.7709	0.5307
0.3	0.0									-1.3274	0.8951	0.5027
	0.3									-1.4279	0.8563	0.5188
	0.6									-1.4892	0.8310	0.5243
	0.9									-1.5595	0.8034	0.5331
	0.6	0.0								-0.8180	0.8967	0.4346
		0.2								-0.9403	0.7994	0.4317
		0.4								-1.4892	0.8310	0.5243
		0.4	0.0							-4.0139	-1.0615	0.9111
			0.5							-1.4892	0.8310	0.5243
			1.0							-1.1883	0.9440	0.5797
			0.5	0.0						-1.4892	0.9121	0.5112
				0.2						-1.4892	0.8594	0.5197
				0.3						-1.4892	0.8310	0.5243
				0.5						-3.1899	-0.3621	0.9832
				0.3	0.2					-1.4892	0.8756	0.3579
					0.3					-1.4892	0.8602	0.4228
					0.5					-1.4892	0.8310	0.5243
					1.0					-3.1899	-0.4175	1.4695
					0.5	0.0				-3.1899	-0.1072	0.8330
						0.2				-3.1899	-0.1447	0.8882
						0.4				-1.4892	0.8310	0.5243
						0.6				-1.4892	0.8467	0.4766
						0.4	0.0			-1.4892	1.1020	0.4743
							0.3			-1.4892	0.8310	0.5243
							0.5			-3.1899	-1.2950	1.1511
							0.3	0.0		-1.1808	0.8163	0.4878
								0.3		-1.3217	0.8221	0.5055
								0.7		-1.4892	0.8310	0.5243
								0.7	0.0	-3.9920	-0.7724	1.1407
									0.5	-1.6072	0.8078	0.5487
									0.9	-1.4892	0.8310	0.5243
									1.2	-1.4470	0.8338	0.5173

Table 2: Numerical values of Skin friction, local Nusselt number and local Sher-wood number.

S	$\frac{T_\infty}{T_w}$	Sr_∞	K	δ_m	σ_s	Du	Sc	Sr	Gb	Z	d	$Re^{\frac{1}{2}}C_f$	$Re^{-\frac{1}{2}}Nu_x$	$Re^{-\frac{1}{2}}Sh_x$

-0.3	0.6	0.8	0.6	0.4	0.5	0.3	0.5	0.4	0.3	0.7	0.9	-2.1853	0.4599	0.5843
-0.2												-2.0684	0.5352	0.5842
-0.1												-1.9627	0.6003	0.5877
0.0												-1.8563	0.6610	0.5919
0.1												-1.7497	0.7174	0.5967
0.2												-1.6276	0.7760	0.5988
0.3	0.0											-1.4892	0.8345	0.5779
	0.3											-1.4892	0.8353	0.5878
	0.6											-1.4892	0.8361	0.5980
	0.8											-1.4892	0.8367	0.6049
	0.6	0.0										-1.4892	0.8374	0.6117
		0.4										-1.4892	0.8368	0.6049
		0.8										-1.4892	0.8361	0.5980
		1.0										-1.4892	0.8358	0.5945
		0.8	0.0									-1.3274	0.9006	0.5840
			0.3									-1.4279	0.8616	0.5954
			0.6									-1.4892	0.8361	0.5980
			0.9									-1.5595	0.8084	0.6033
			0.6	0.0								-0.8180	0.9022	0.5202
				0.2								-0.9403	0.8043	0.4992
				0.4								-1.4892	0.8361	0.5980
				0.4	0.0							-4.1749	-1.2211	0.9025
					0.5							-1.4892	0.8361	0.5980
					1.0							-1.1883	0.9492	0.6590
					0.5	0.0						-1.4892	0.9121	0.5961
						0.2						-1.4892	0.8629	0.5972
						0.3						-1.4892	0.8361	0.5980
						0.3	0.2					-1.4892	0.8768	0.3960
							0.3					-1.4892	0.8624	0.4745
							0.5					-1.4892	0.8361	0.5980
							1.0					-1.4892	0.7749	0.8295
							0.5	0.0				-3.1899	-0.1059	0.9325
								0.2				-3.1899	-0.1422	0.9386
								0.4				-1.4892	0.8361	0.5980
								0.6				-1.4892	0.8554	0.5976
								0.4	0.0			-1.4892	1.1080	0.5758
									0.3			-1.4892	0.8361	0.5980
									0.5			-3.1899	-1.2923	1.1021
									0.3	0.0		-1.1808	0.8212	0.5595
										0.3		-1.3217	0.8271	0.5779
										0.7		-1.4892	0.8361	0.5980
										0.7	0.0	-1.8173	0.7658	0.6580
											0.5	-1.6072	0.8129	0.6197
											0.9	-1.4892	0.8361	0.5980
											1.2	-1.4470	0.8389	0.5911

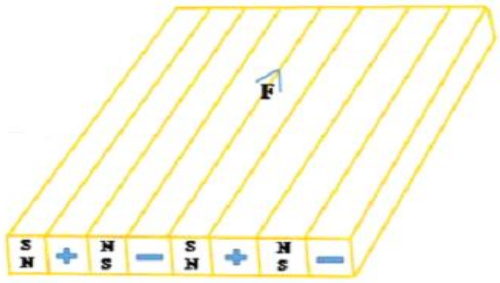

Fig. 1: Physical configuration of the flow.

(a) **(b)**

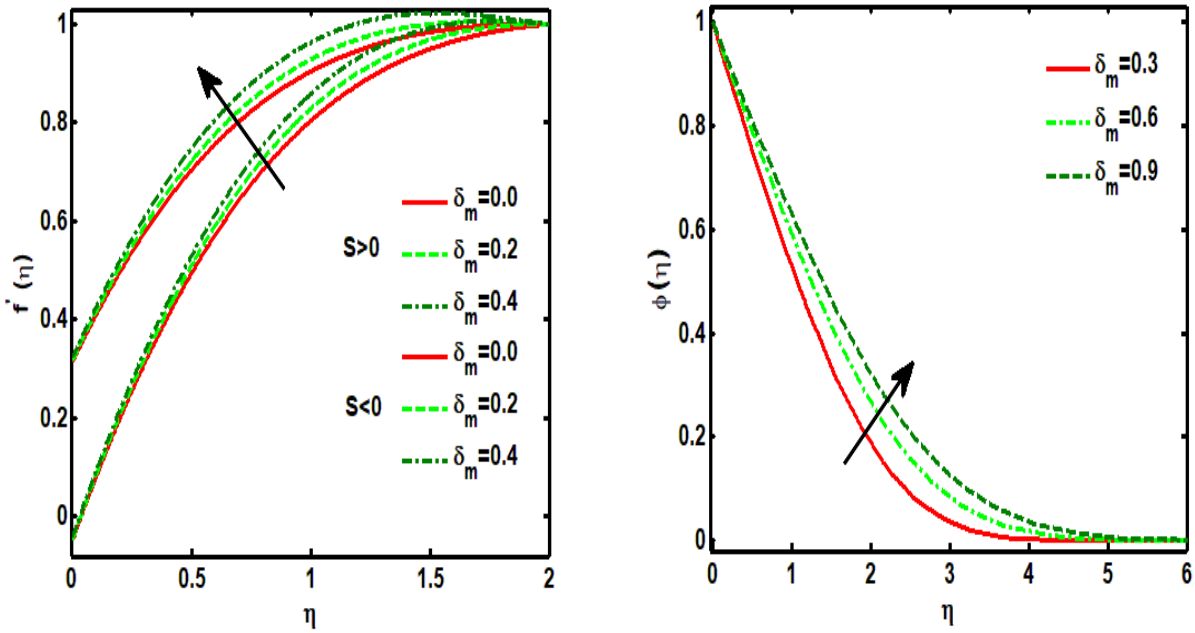

Figs 2: Effect of viscoelastic parameter δ_m on (a) Normalized fluid velocity, (b) Concentration field. $\left(Pr = 0.5, \sigma_s = 0.1, Du = 0.3, Sc = 0.2, Sr = 0.3, Ec = 0.3, K = 0.2, Z = 0.2, d = 0.2, S = -0.2, 0.2\right)$

(a) **(b)**

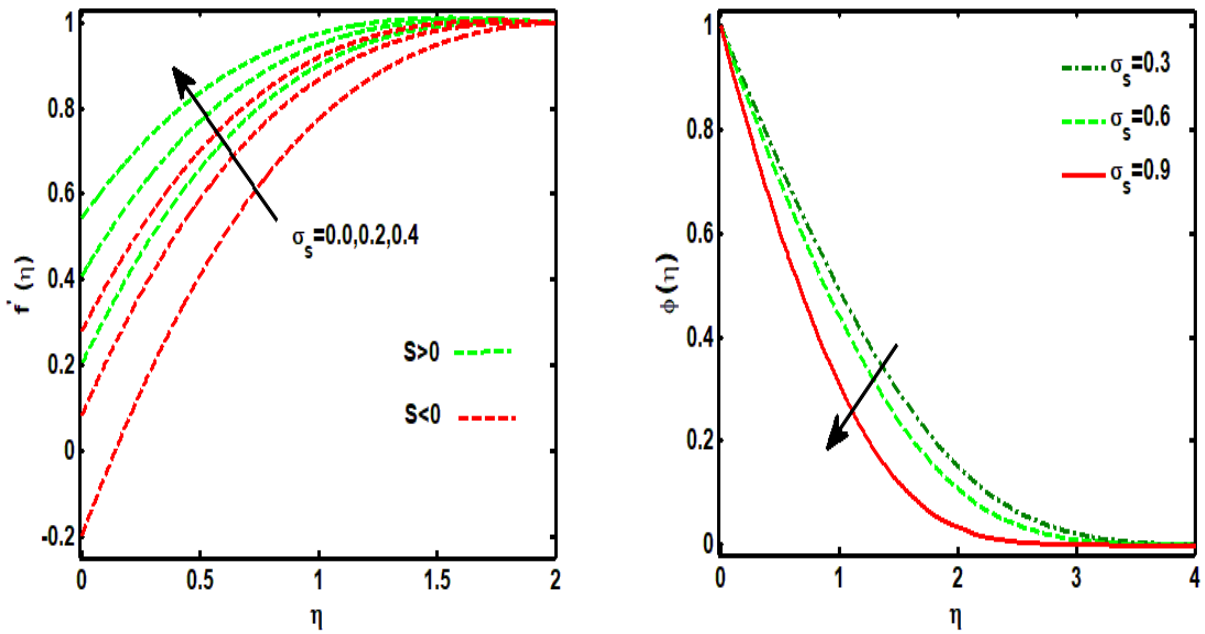

Figs 3: Effect of Slip condition σ_s on (a) Normalized fluid velocity,(b) Concentration field. $\left(Pr = 0.5, \delta_m = 0.2, Du = 0.3, Sc = 0.2, Sr = 0.3, Ec = 0.3, K = 0.2, Z = 0.2, d = 0.2, S = -0.2, 0.2\right)$.

(a) **(b)**

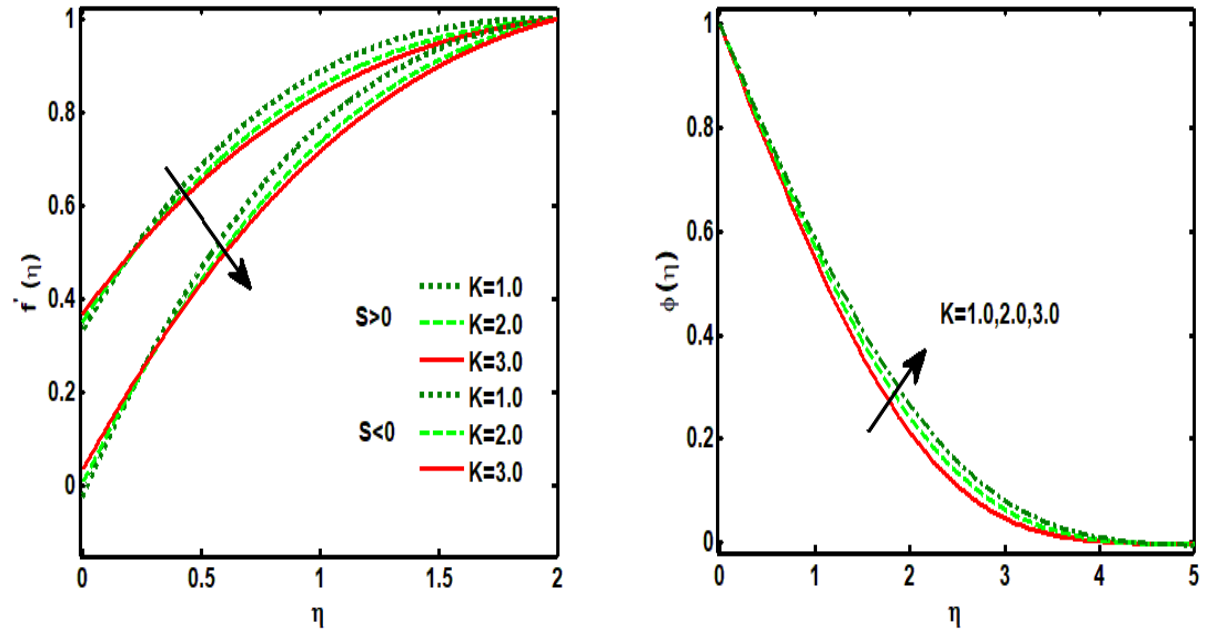

Figs 4: Effect of material parameter K on (a) Normalized fluid velocity,(b) Concentration field. $\left(Pr = 0.5, \delta_m = 0.2, \sigma_s = 0.1, Du = 0.3, Sc = 0.2, Sr = 0.3, Ec = 0.3, Z = 0.2, d = 0.2, S = -0.2, 0.2\right)$.

(a) **(b)**

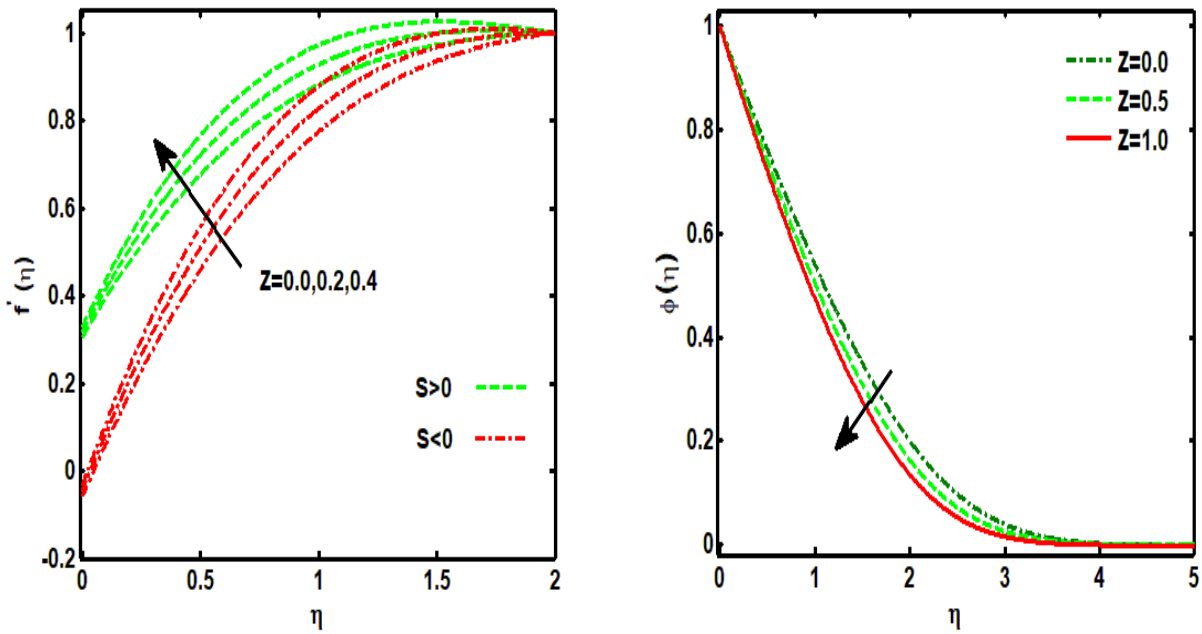

Figs 5: Effect of Modified Hartman number Z on (a) Normalized fluid velocity,(b) Concentration field. $\left(Pr=0.5,\delta_m=0.2,\sigma_s=0.1,Du=0.3,Sc=0.2,Sr=0.3,Ec=0.3,K=0.2,d=0.2,S=-0.2,0.2\right)$.

(a) **(b)**

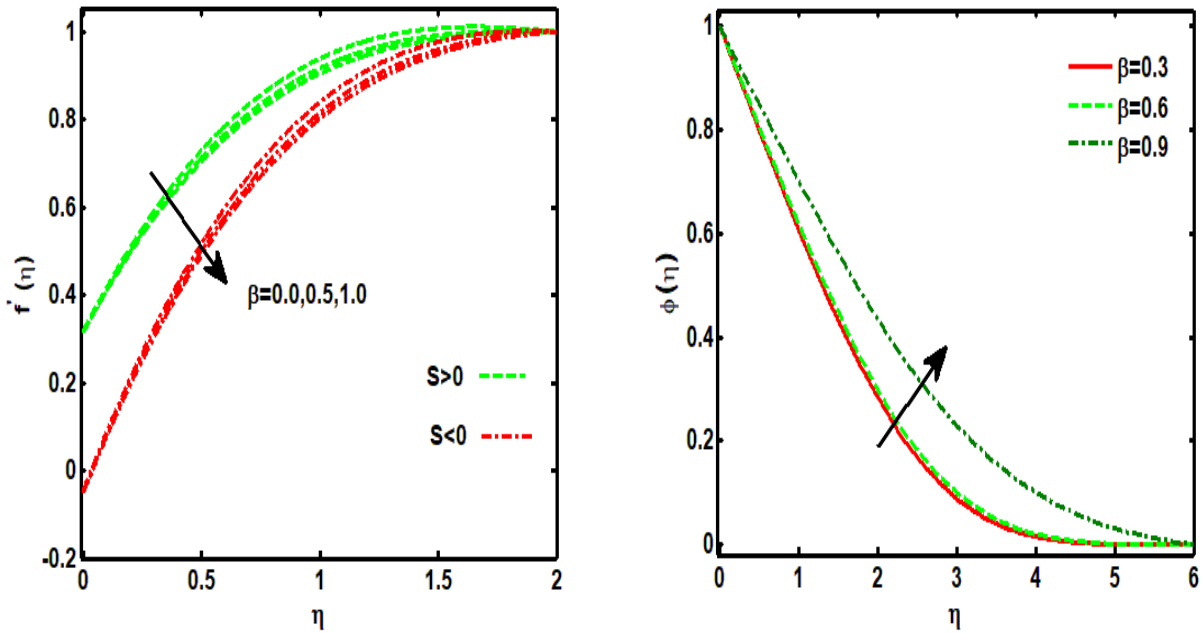

Figs 6: Effect of dimensionless parameter β on (a) Normalized fluid velocity,(b)Concentration field. $\left(Pr=0.5,\delta_m=0.2,\sigma_s=0.1,Du=0.3,Sc=0.2,Sr=0.3,Ec=0.3,K=0.2,Z=0.2,S=-0.2,0.2\right)$.

(a) **(b)**

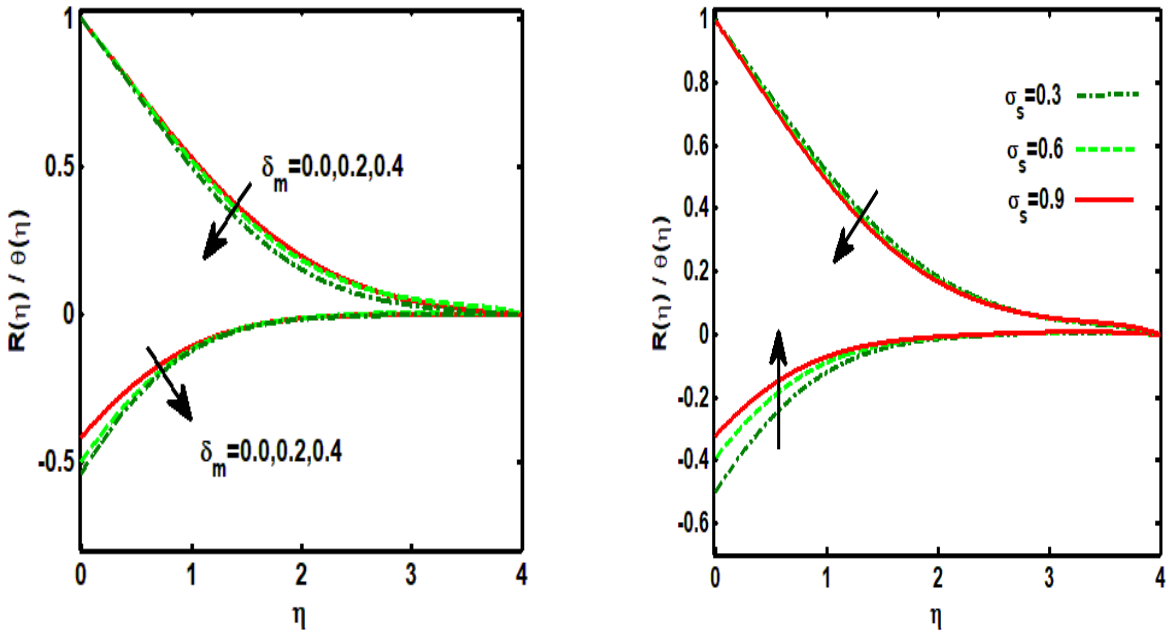

Figs 7: Effect of (a) viscoelastic parameter δ_m (b) Slip condition σ_s on $R(\eta)$ and $\theta(\eta)$. $(Pr = 0.5, \delta_m = 0.2, \sigma_s = 0.3, Du = 0.3, Sc = 0.2, Sr = 0.3, Ec = 0.3, K = 0.2, Z = 0.2, S = -0.2, 0.2)$.

(a) **(b)**

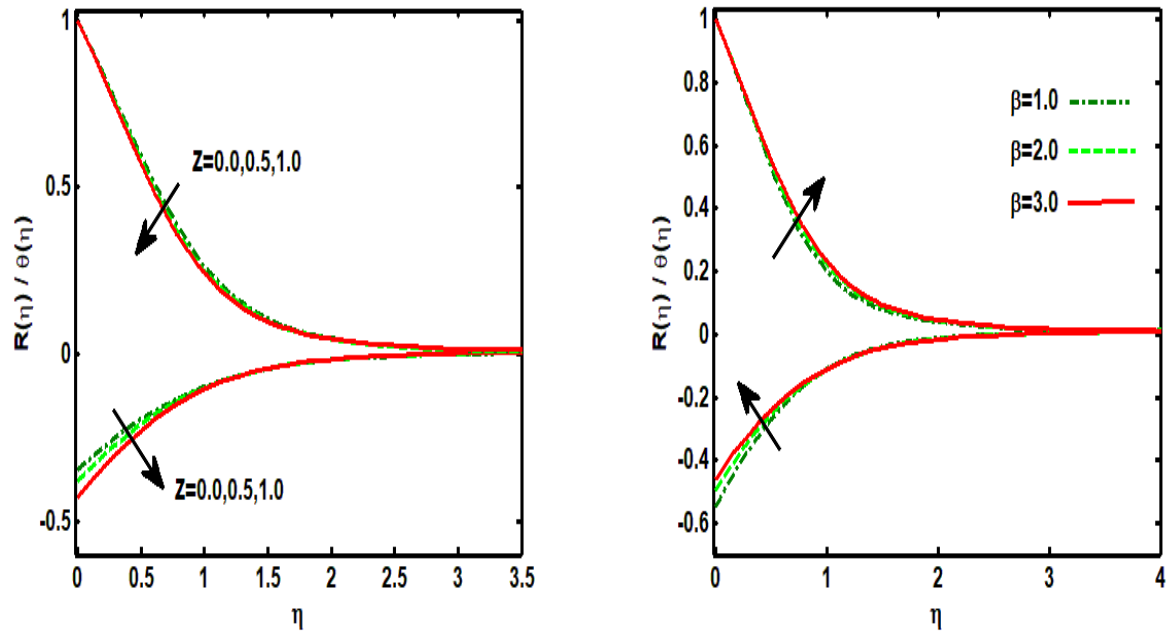

Figs 8: Effect of (a) Modified Hartman number Z (b) dimensionless parameter β on $R(\eta)$ and $\theta(\eta)$. $(Pr = 2.0, \delta_m = 0.5, \sigma_s = 0.5, Du = 0.3, Sc = 0.5, Sr = 0.3, Ec = 0.4, K = 0.5, Z = 2.0, S = 0.2)$.

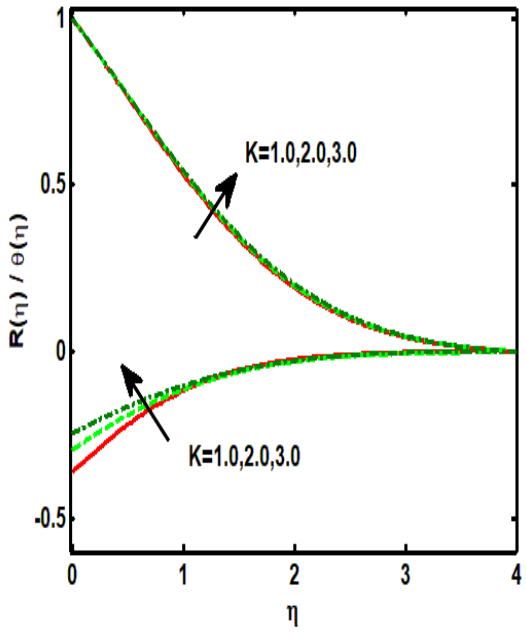

Figs 9: Effect of Material parameter K on $R(\eta)$ and $\theta(\eta)$. $(Pr = 0.5, \delta_m = 0.2, \sigma_s = 0.3, Du = 0.3, Sc = 0.2, Sr = 0.3, Ec = 0.3, K = 0.2, Z = 0.2, S = 0.2)$.

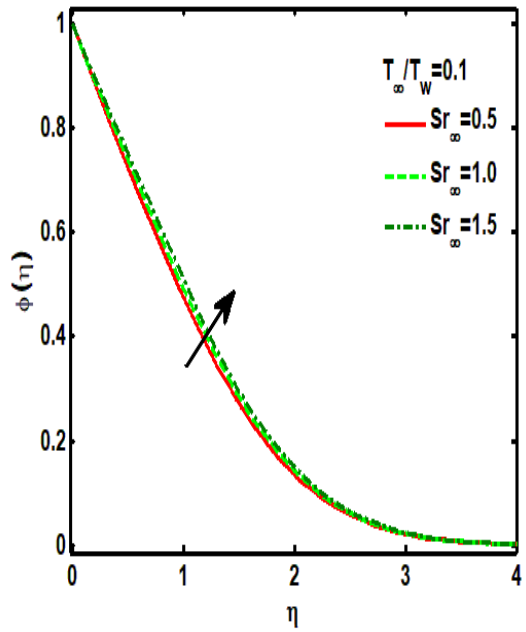

Fig 10: The parameter Sr_∞ associated with the micro-particle size has visible effect on the concentration field with large imposed temperature differences $\frac{T_\infty}{T_w}$. $(Pr = 2.0, \delta_m = 0.5, \sigma_s = 0.5, Du = 0.3, Sc = 0.5, Sr = 0.3, Ec = 0.4, K = 0.5, Z = 1.0, S = 0.2)$.

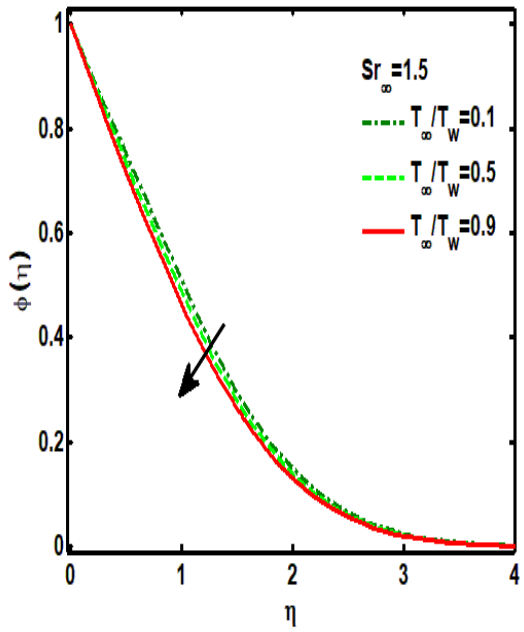

Fig 11: Effect of variable temperature differences $\frac{T_\infty}{T_w}$ on the concentration field for large particle. $\left(Pr = 2.0, \delta_m = 0.5, \sigma_s = 0.5, Du = 0.3, Sc = 0.5, Sr = 0.3, Ec = 0.4, K = 0.5, Z = 1.0, S = 0.2\right)$.